Full scale rotor blade deformation measurements in comparison with aeroelastic simulations based on measured high-resolution wind fields

Full scale rotor blade deformation measurements in comparison with aeroelastic simulations based on measured high-resolution wind fields

S Lehnhoff [1], A P Kidambi Sekar [2], M F van Dooren [2], M Kühn [2] and J R Seume [1]

[1] ForWind - Center for Wind Energy Research, Leibniz Universität Hannover, Institute of Turbomachinery and Fluid Dynamics - TFD, An der Universität 1, 30823 Garbsen, Germany
[2] ForWind - Center for Wind Energy Research, University of Oldenburg, Küpkersweg 70, 26129 Oldenburg, Germany

E-mail: lehnhoff@tfd.uni-hannover.de

Abstract. Aeroelasticity is one of the biggest challenges in wind turbine rotor design, as the length of rotor blades increases which comes along with a slenderer design. The knowledge of the aeroelastic turbine behavior is of great importance. A comparison to field measurements is of huge importance when validating aeroelastic tools. However, the measurement of deformation and torsion in the field is not trivial and the conduction of realistic post-test simulations is a challenge. One crucial factor for these simulations is the wind field, which needs to be captured in a high spatial and temporal resolution. In this paper, the results of deformation measurements conducted in the field with an optical measurement method called Digital Image Correlation (DIC) on one rotor blade will be shown and compared to aeroelastic post-test simulations using highly resolved wind fields measured with a SpinnerLidar.

1. Introduction

Aeroelasticity is one of the biggest challenges in wind turbine rotor design. As the market demands a reduction of cost for nominal power, wind turbine manufacturers are driven to build bigger wind turbines. This comes along with a growth of the rotor blades that become longer and slenderer at the same time. The knowledge of the aeroelastic turbine behavior in the field is of great importance.

However, it is not trivial measure deformation and torsion in the field. And just as important as good field measurement data are realistic post-test simulations for validation. One crucial factor for these simulations is the wind field, which needs to be captured with high spatial and temporal resolution.

In the project SmartBlades2, a new rotor with bend-twist coupled blades was designed for a 700 kW wind turbine. The blades were manufactured and analyzed with high detail and effort, so that the blades' structure is well characterized. In addition to this, the manufactured blades were equipped with many different measurement techniques and installed on the Controls Advanced Research Turbine (CART3) at the test site of the National Renewable Energy Laboratory

(NREL) in Boulder. During a field measurement campaign in January 2019, field data was recorded and will be used for validation of design tools.

A validation of aeroelastic simulations of wind turbines is usually based on a huge database of long-term measurements, as e.g. found in [1] and [2]. In this paper, the measurement results of rotor blade deformations are based on an optical measurement method called Digital Image Correlation (DIC). The measurement duration of this method is usually not longer than ten minutes, due to changes in illumination conditions in the field. This requires a highly-resolved description of the actual prevailing wind conditions for a validation of aeroelastic simulations based on those measurements.

One way to improve the characterization of the wind is the integration of LiDAR data into aeroelastic simulations. As mentioned in [3], it is beneficial to increase the detail of inflow information to achieve a better accuracy in the simulation of wind turbine fatigue loads. In [4], a detailed analysis of the implementation of LiDAR-based inflow information is given and it turns out that the load estimation uncertainty decreases in most of the cases if LiDAR-based signals are used, in comparison to met mast data.

In this paper, the results of deformation measurements conducted with DIC on one rotor blade are presented and compared to aeroelastic post-test simulations using highly-resolved wind fields measured with a SpinnerLidar. A method for the reconstruction of realistic wind fields for aeroelastic simulations based on SpinnerLidar data will be presented. The derived wind field is compared to actual measured wind conditions from anemometers for a first verification of the wind field fed into the simulation. Afterwards, a comparison of simulated and measured wind turbine conditions and blade tip deformations is shown.

2. Methodology

This part describes the experimental setup, which was used for the investigations, shortly introduces the feasibility of DIC for the application on full scale wind turbines and explains the data processing of the LiDAR data for implementation in the aeroelastic simulations.

2.1. Experimental setup

In this measurement campaign, the test wind turbine was equipped with many different measurement techniques. To name a few, strain gauges in all rotor blades at different radial positions, an optical measurement system inside the blades ([5]) as well as outside the blades (in form of speckles for DIC) on the pressure side for the detection of rotor blade deformation and torsion were installed. An overview of the spatial positioning of the turbine and external instrumentation is given in Figure 1.

The wind field was investigated with a met mast equipped with cup anemometers at different heights in a distance of approximately 2.0 D and a SpinnerLidar was installed on top of the nacelle of the turbine by ForWind Oldenburg. The SpinnerLidar measures the wind velocity in a distance of approximately 1.4 D upstream of the turbine with high spatial and temporal resolution. A spherical area with a diameter of approximately 60 m is scanned with 624 measurement points at a scan rate of 312 Hz. This results in a total scan-rate of the area in front of the turbine of 0.5 Hz. More information on the LiDAR can be found in [6]. Additionally, a cup anemometer on top of the nacelle was installed.

2.2. Digital Image Correlation

The term DIC describes an optical measurement method that can detect deformation and/or motion of certain objects [8]. To apply DIC on wind turbines, a random speckle pattern needs to be applied on the surface of the rotor blades, as shown in Figure 2. The wind turbine is then monitored with a stereo camera system from the ground. Based on these pictures, the

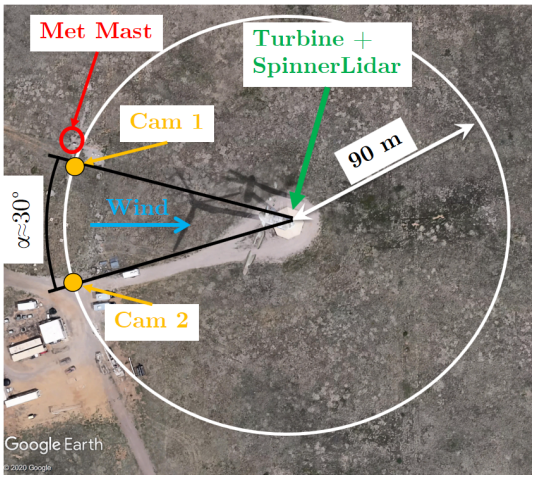

Figure 1. Experimental setup at the National Wind Technology Center (NWTC) of NREL in Boulder, Colorado, USA

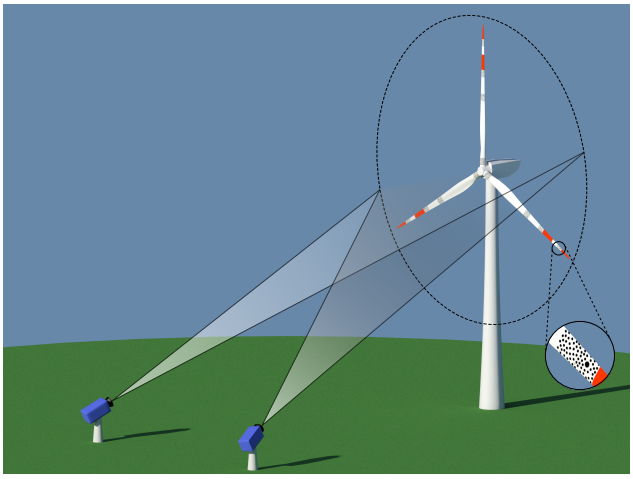

Figure 2. Measurement setup for DIC measurements on wind turbines [7]

deformation and torsion of the blades can be determined in those areas, where the speckles were applied. More information on the functionality of DIC can be found in [8].

DIC was tested and developed over the last few years by ForWind Hanover for full scale wind turbine applications ([9], [10], [7]) and can be considered a suitable measurement technique for the detection of rotor blade deformations of full scale wind turbines. The commercial software Vic3D, a DIC software from Correlated Solutions, Inc., is used for the investigations [11]. A first comparison with aeroelastic simulations based on 10-minute averaged statistical wind conditions was already shown in [12]. It turned out that a direct comparison of measurements and those simulations is not easy to implement, and the integration of the prevailing wind condition is of huge importance for a comparison of measurements with simulations.

2.3. Wind field reconstruction and implementation in aeroelastic simulations

The SpinnerLidar measures the line-of-sight (v_{los}) projection of the 3-dimensional wind speed along the laser beam which can be represented as:

$$v_{\mathrm{los}} = \cos\chi\cos\delta \cdot u + \sin\chi\cos\delta \cdot v + \sin\chi \cdot w \tag{1}$$

where χ and δ are the azimuth and elevation angle of the laser beam and u, v, w are the 3D wind velocity components at the measurement point. As the longitudinal component (u) is much higher than the lateral and vertical component, it is a reasonable assumption that the longitudinal wind speeds can be obtained from the SpinnerLidar by setting $v, w = 0$ in equation 1. The wind field measured by a SpinnerLidar, which is a combination of v_{los} speeds at the different measurement points, can be represented as a combination of wind field parameters as defined in [13]:

$$v_{\mathrm{los}}(y,z) = (u_o + s_h y + s_v z) \begin{bmatrix} \cos(\delta_v)\cos(\delta_h) \\ \cos(\delta_v)\sin(\delta_h) \\ \sin(\delta_v) \end{bmatrix} \tag{2}$$

The mean wind speed u_0 is inclined to the rotor plane with the wind directions δ_{h} and δ_{v}. The shear is calculated as the linearly changing wind speed along the horizontal (y) and vertical (z) axes. A simplified three-parameter model is created by assuming that both the vertical up-flow and the horizontal shear are zero and an exponential shear parameter (α) is included.

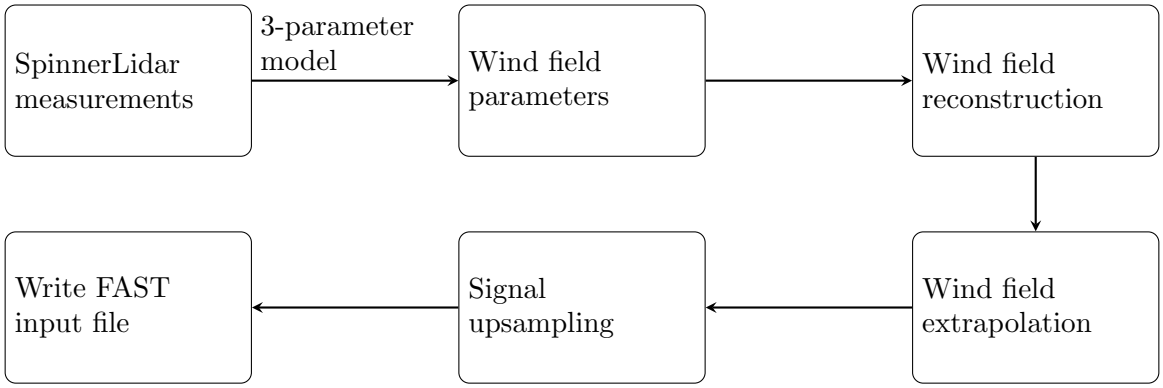

Figure 3. Methodology for creating FAST input files based on SpinnerLidar measurements [15]

For performing aeroelastic simulations with the wind inflow, LiDAR measurements cannot be directly used as an input wind field due to the directional bias effects and the spatial-temporal measurement limitations of the device. The SpinnerLidar measures the inflow at a focus distance of 60 m upstream of the rotor in a spherical plane of 60 m diameter. As this scan pattern is not enough to capture the wind field variations from the tower bottom to the upper blade tip position, this data needs to be extrapolated from the LiDAR measurements.

To generate the missing data for the aeroelastic wind field input file, the results of the three-parameter model are used. The wind field parameters u_0, α and δ_h are used to generate the wind velocities at grid points outside the 60 m diameter measurements from the SpinnerLidar. For those points inside the rosette pattern of the SpinnerLidar, the longitudinal component of the velocity u is simply calculated by projecting the line-of-sight velocity v_los to the horizontal direction. For extrapolating the velocities outside the SpinnerLidar measurement plane, a power law extrapolation scheme based on the shear parameter α is used. For those points outside the rosette pattern and in the hub height horizontal line of the grid, the longitudinal component of the wind u is calculated based on the mean wind speed (u_0), the horizontal inflow direction δ_h and the location of the point with respect to its horizontal position. The velocity on the grid points on the vertical plane are calculated based on the shear parameter α from the three-parameter model. The lateral component of the wind v is calculated based on the longitudinal component u and the instantaneous yaw misalignment δ_h. With this extrapolation scheme, full grid information from the tower bottom to the blade tip is obtained, sampled at 0.5 Hz.

As specified in [14], for performing aeroelastic simulations, the wind fields must be generated with a time step of at least 0.05 s (typically a 20 Hz sampling rate of a TurbSim file) in order to obtain reasonable results. The SpinnerLidar data is up-sampled to 20 Hz by means of an anti-aliasing finite impulse response (FIR) low-pass filter in order preserve the energy content in the signal. Finally, the time series for the velocities at the grid points are written in the form of a 4D array in a .bts file and used as an input wind file for FAST. The entire process of implementing the SpinnerLidar data in FAST is shown in Figure 3. Figure 4 shows an example of the wind field generated from SpinnerLidar measurements.

Both wind measurements from the LiDAR and the met mast are corrected by the influence of the axial induction with a factor of $a = 0.3$, according to the vortex sheet theory as described in [16].

The aeroelastic model is implemented in OpenFAST [17]. The blade information is derived from the design phase of the blade development and was set up by Fraunhofer IWES. The loads on the blades are calculated with ElastoDyn.

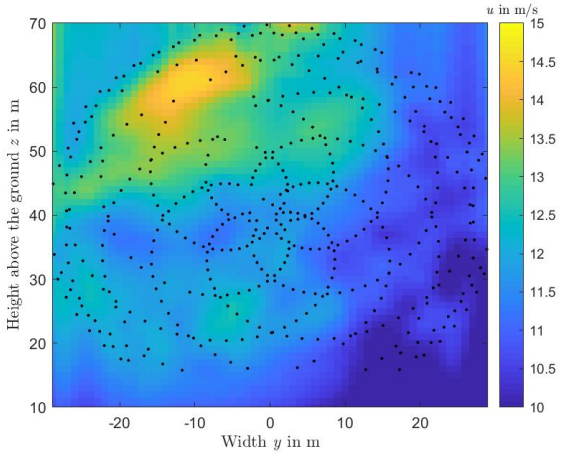

Figure 4. Exemplary wind field reconstructed from SpinnerLidar data

3. Results

This section compares the wind fields implemented in OpenFAST with measured wind conditions to evaluate the quality of the implementation method. Afterwards, the simulated turbine conditions in form of rotational speed and pitch angle are compared to measured data. This is followed by a comparison of the simulated out-of-plane (OoP) and in-plane (IP) deformation at the blade tip with DIC measurement results. The simulations were run for a five minute time series, whereof only the last three minutes will be shown to keep the overview.

3.1. Wind simulation vs. measurements

Figure 5 shows the wind speed at the wind turbine nacelle from measurements and derived wind data. From the measurements, the nacelle anemometer and one measurement point of the LiDAR at the horizontal position of the turbine in wind direction at hub height is extracted. The derived wind field (as .bts file) fed into OpenFAST is shown, as well as the output from the simulation at the same position as the LiDAR data point. The nacelle anemometer data is not corrected by the induction factor and is only used to demonstrate the similarity of the trend of all curves.

The time signals of all data sets were synchronized according to the nacelle anemometer, to compare all results directly to the simulations. The nacelle anemometer shows a clear offset in comparison with the other values, which can be explained by the effect of axial induction during power production of the turbine, as the anemometer was not corrected by this factor. The LiDAR data has several gaps, which are caused by the blockage of the laser beam by the rotating blades in front of the LiDAR. The .bts file is based on all LiDAR measurement points, thus it has no gaps and clearly follows the LiDAR signal. The wind exported from the simulation is remarkably close to the .bts file results, which are also shown as a scatter plot in Figure 6 with a high value of the linear regression fit coefficient R^2 of 0.914. Thus, the .bts file results can be considered nearly identical to the wind exported from the simulation and represents the simulation results in the following Figure. The trends of all curves are similar, which proves that the wind data fed into OpenFAST correspond to the actual prevailing wind conditions at hub height. Comparisons of time slots when the turbine is in stand-still mode are in particularly good agreement, which proves this statement.

Figure 7 shows time series of the met mast anemometer at hub height in comparison with one measurement point of the LiDAR, .bts file and simulation at the same height and as close as possible to the same horizontal position. The met mast data is corrected so that it shows

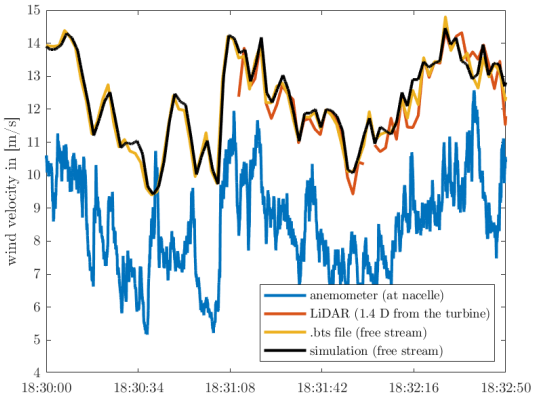

Figure 5. Wind velocity at the position: horizontal: wind turbine, vertical: hub height

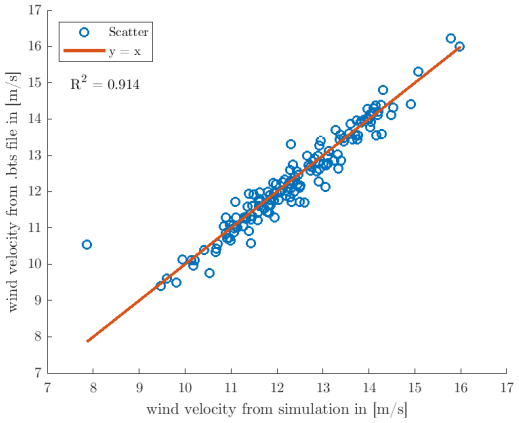

Figure 6. Comparison of wind field from simulation and .bts file at the wind turbine nacelle position at hub height

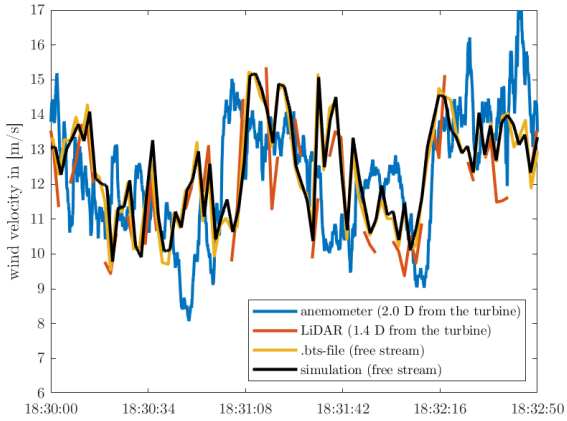

Figure 7. Wind velocity at the position: horizontal: met mast, vertical: hub height

only the wind propagating in turbine direction. The wind signals from the LiDAR, .bts file and simulation are in particularly good agreement, while the anemometer shows small differences. This could be caused by a difference in the actual position of the measurement points, as the LiDAR did not measure exactly at the same horizontal position as the met mast. Another factor could be the influence of the turbulence on the wind. As the LiDAR does not measure in the same distance as the met mast, the wind propagating to the turbine could be influenced by local turbulence.

In summary, the simulated wind conditions are in good agreement with the measured wind conditions and the wind field that is fed into OpenFAST can be considered realistic and synchronized with turbine measurement data.

3.2. Wind turbine operational data simulation vs. measurements

Given that the wind field can be considered realistic, a comparison of measured and simulated turbine conditions can be made.

Figure 8 shows a comparison of measured and simulated pitch angle. The DIC measurements

are in particularly good agreement with the supervisory control and data acquisition (SCADA) data of the turbine. The simulated pitch angle shows the same trend as SCADA and DIC. However, there is an offset in the maximum simulated pitch angle of approximately 5°, which is significantly lower than in reality. A hypothesis explaining the differences is given below. This has without doubt a big impact on the following comparisons. Nevertheless, the regions of fixed and changing pitch angle are in the same time slots for all curves proving that the simulated turbine reacts to changes of the wind conditions and shows the same qualitative behavior.

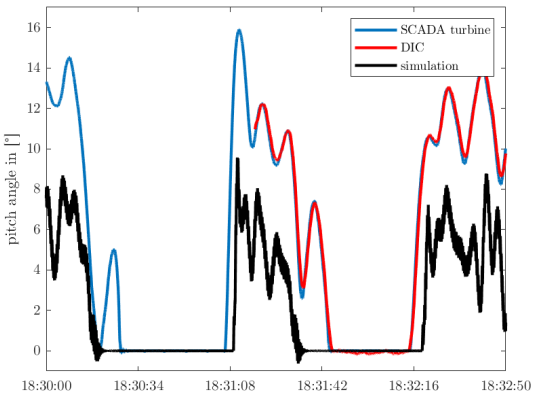

Figure 8. Pitch angle from simulation and experiment

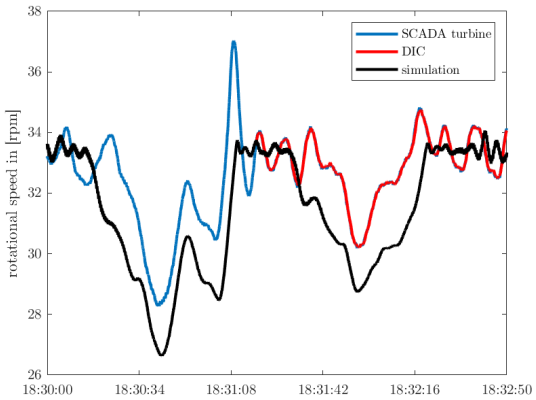

Figure 9. Rotational speed from simulation and experiment

Consequently, similar observations can be made regarding the rotational speed in Figure 9. It can be seen that the nominal rotational speed for both simulation and measurement has the same mean value of around 33 *rpm* as defined by the controller. When the wind speed decreases, the turbine behavior shows the same trend for all curves. However, there is a clear offset of the minimum rotational speed of approximately 2 *rpm*. The point of time, when the turbine starts to set the pitch angle to 0° has a big influence on the rotational speed, as it indicates a decrease in wind speed. The simulation model starts earlier to set the pitch to 0° and thus the rotational speed decreases earlier than in reality and therefore needs more time to recover to nominal rotational speed.

In summary, the simulated turbine seems to be more sensitive to a decrease in wind speed than the real turbine, which can have several reasons. One obvious reason is a difference between the simulation model and the real turbine, as it is a challenge to build a model which represents the real turbine. The simulation model which is used here is based on blade information out of the design phase and will be updated in the future to represent a more realistic simulation model.

However, the wind field does also have a huge impact on the turbine behaviour and needs to be investigated in more detail to make sure that it reproduces the reality. In a short study, the wind conditions were modified by different offset values to estimate the influence of a change in wind conditions on the simulation results. The results for an offset of $+0.75\ m/s$ are shown in Figures 10 and 11. This offset brings all curves for the measured and simulated pitch angle and rotational speed significantly closer together. This demonstrates that the wind field has a big impact on the turbine behavior and needs to be validated as accurately as possible to serve as a base for aeroelastic simulations. As the impact of an update of the aeroelastic model on the simulation results cannot be estimated at this point of time, it is unclear which source of error is more likely in this case. This is subject to further investigation.

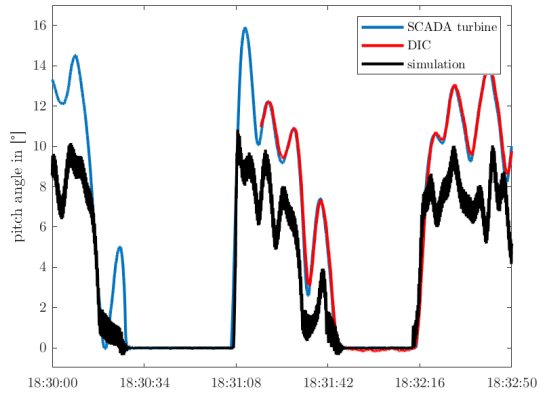

Figure 10. Pitch angle from simulation and experiment; wind conditions in simulation modified by + 0.75 m/s

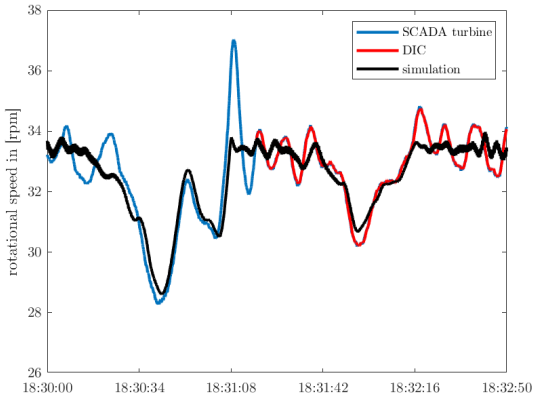

Figure 11. Rotational speed from simulation and experiment; wind conditions in simulation modified by + 0.75 m/s

3.3. Deformation simulation vs. DIC measurement

Lastly, DIC measurements are compared to deformations of the simulation model.

Figures 12 and 13 show the OoP and IP deformation of DIC and simulation of a 1:30 minutes time series, which were all reduced by their moving average over one rotor revolution for an improved comparability.

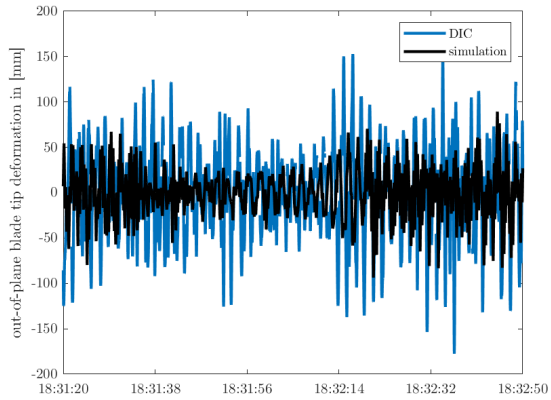

Figure 12. OoP deformation at the blade tip

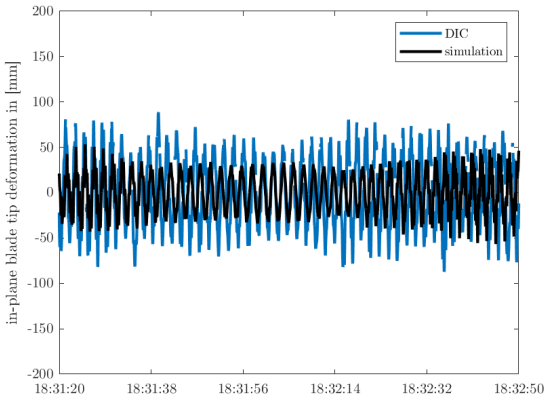

Figure 13. IP deformation at the blade tip

Both plots show that the amplitude measured with DIC is significantly higher when compared to the deformation simulations, which might have the same reasons as explained at the end of section 3.2. However, all curves show a similar behavior. The amplitude of deformation at the beginning and at the end of the time slot has a similar value, while in the middle it is clearly decreased. This can be analyzed in more detail by looking at the next figures.

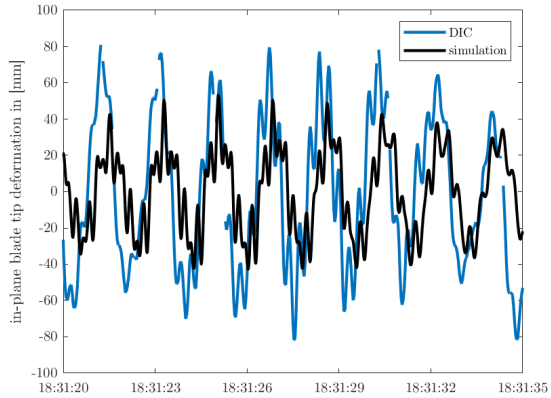

Figure 14. IP deformation at the blade tip - Zoom 1

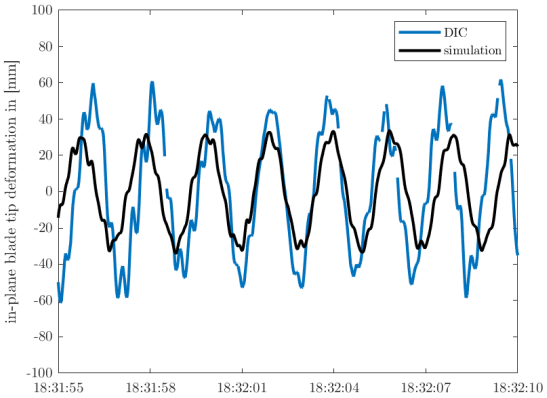

Figure 15. IP deformation at the blade tip - Zoom 2

These plots show the IP deformation for a period of 15 seconds at the beginning (Figure 14) and in the middle of the time series (Figure 15). In Figure 14, a lot of additional small peaks on the basic vibration curve can be observed in the IP vibration curve. During this time slot, the additional vibration seems to be well developed when compared to the next time slot in Figure 15. Here, both curves - for simulation and measurement - show the basic vibration with only minor additional peaks. The time slots for strong or damped additional vibration seem to be well predictable with the simulation model, even if the amplitude of vibration is different.

This shows that a direct comparison of measurement and simulation seems to be feasible based on fed-in wind data measured with a SpinnerLidar.

4. Conclusions

This paper shows results from a direct comparison of aeroelastic simulations, based on a wind field obtained from SpinnerLidar measurements, in comparison with deformation measurements, based on DIC, in a time series of the length of 1:30 minutes. The method for the direct integration of SpinnerLidar data into OpenFAST is described as well as the optical measurement method.

The wind field read into OpenFAST is very similar to the measured one in front of the turbine due to the direct transfer of measured values. This can be observed from comparisons with measured wind speeds from cup anemometers on a met mast and on the nacelle of the turbine. First comparisons of simulation results to measurements show that the trend of the time-resolved turbine behavior, exemplarily shown in form of pitch angle and rotational speed, can be reproduced with this method. The trend of simulated deformations is similar to that measured with DIC. Although the amplitude measured with DIC is significantly higher, the time slots of well-developed or damped additional vibrations can be reproduced from the simulations.

The differences between these data sets can have several different causes. One highly probable cause is the difference between the simulation model and the real turbine, as the model is based on rotor blade data obtained from the design process of the blades. The model runs with ElastoDyn at this point of time which does not take into account torsional deformation of the blades, which needs to be updated to reproduce the behavior of bend-twist coupled blades. Another big factor is the wind field which has a huge impact on the turbine behavior as shown in a short modification study. This needs to be investigated in more detail to make sure that it reproduces the reality. These points will be considered for further investigation.

In summary, this is a successful first step for a direct comparison of measurements and

simulations and shows that SpinnerLidar data can make a valuable contribution when validating aeroelastic codes.

Acknowledgments
The auhtors gratefully acknowledge the financial funding from the Federal Ministry for Economic Affairs and Energy (BMWi) of Germany for the joint project SmartBlades2 (0324032A-H). We thank our colleagues at TFD, University of Oldenburg and Fraunhofer IWES for the valuable discussions concerning the results of this work. We also thank the technical staff from NREL and TFD for their support during the measurement campaign. We want to thank Fraunhofer IWES, in person Paul Feja for building and providing the FAST-model of the wind turbine and Tobias Meyer for developing and providing the controller of the turbine. In the end, we want to thank the whole SmartBlades2 consortium for the organization and realization of the measurement campaign.

References
[1] Guntur S, Jonkman J, Sievers R, Sprague M, Schreck S and Wang Q 2017 *A validation and code-to-code verification of FAST for a megawatt-scale wind turbine with aeroelastically tailored blades* Wind Energy Science 2:443-468
[2] Paulsen U S, Gomiero M, Larsen T J and Benini E 2018 *Load validation of aero-elastic simulations with measurements performed on a 850 kW horiztonal-axis wind turbine* Journal of Physics: Conf. Series 1037 062023
[3] Pedersen M M, Larsen T J, Madsen H A and Larsen G C 2019 *More accurate aeroelastic wind-turbine load simulations using detailed inflow information* Wind Energy Science 4:303-323
[4] Dimitrov N, Borraccino A, Pena A, Natarajan A and Mann J 2019 *Wind turbine load validation using lidar-based wind retrievals* Wind Energy 22:1512-1533
[5] Nidec SSB Wind Systems GmbH 2020 More than a well-rounded solution: Bladevision Brochure URL `https://www.ssbwindsystems.de/pdf/SSB_Wind_Broschuere_BladeVision_EN.pdf`
[6] Sjöholm M, Pedersen A T, Angelou N, Foroughi Abari F, Mikkelsen T, Harris M, Slinger C and Kapp S 2013 *Full two-dimensional rotor plane inflow measurements by a spinner-integrated wind lidar* Poster session presented at European Wind Energy Conference Exhibition 2013, Vienna, Austria
[7] Winstroth J and Seume J R 2015 *Error Assessment of Blade Deformation Measurements on a Multi-Megawatt Wind Turbine Based on Digital Image Correlation* Proceedings of the ASME Turbo Expo GT2014-43622
[8] Sutton M A, Orteu J J and Schreier H 2009 *Image Correlation for Shape, Motion and Deformation Measurements: Basic Concepts,Theory and Applications* Springer US ISBN 978-0-387-78747-3
[9] Winstroth J and Seume J R 2014 *Wind Turbine Rotor Blade Monitoring Using Digital Image Correlation: Assessment on a Scaled Model* 32nd ASME Wind Energy Symposium 13-17 January 2014, National Harbor, Maryland
[10] Winstroth J and Seume J R 2014 *Wind Turbine Rotor Blade Monitoring Using Digital Image Correlation: 3D Simulation of the Experimental Setup* EWEA 2014 10-13 March 2014, Barcelona, Spain
[11] Correlated Solutions, Inc 2020 Deformation measurement solutions Brochure URL `https://www.correlatedsolutions.com/wp-content/uploads/2013/10/Vic-3D-Brochure.pdf`
[12] Winstroth J, Schoen L, Ernst B and Seume J R 2014 *Wind Turbine Rotor Blade Monitoring Using Digital Image Correlation: A Comparison to Aeroelastic Simulations of a Multi-Megawatt Wind Turbine* Journal of Physics: Conference Series 524 012064
[13] Kapp S and Kühn M 2014 *A Five-Parameter Wind Field Estimation Method Based on Spherical Upwind Lidar Measurements* Journal of Physics: Conference Series 555 012112
[14] Jonkman J M and Buhl Jr M L 2005 FAST Users Guide Tech. rep. NREL
[15] Kidambi Sekar A P and van Dooren M F 2019 SmartBlades 2.0, Deliverable 1.3.15.3: Analyse, Korrelationsanalyse turbulenter Einströmung zu Anlagenlasten Tech. rep. ForWind - University of Oldenburg
[16] Medici D, Ivanell S, Dahlberg J A and Alfredsson P H 2011 *The upstream flow of a wind turbine: blockage effect* Wind Energy vol. 14, pp. 691-697
[17] NWTC Information Portal (OpenFAST). `https://nwtc.nrel.gov/OpenFAST` ; Last modified: 2018-01-05; Accessed: 2020-02-13